Atmospheric
Chemistry
and Physics

Open Access

# Characterization of long-term and seasonal variations of black carbon (BC) concentrations at Neumayer, Antarctica

**R. Weller**[1], **A. Minikin**[2], **A. Petzold**[2,*], **D. Wagenbach**[3], and **G. König-Langlo**[1]

[1]Alfred Wegener Institute for Polar and Marine Research, Am Handelshafen 12, 27570 Bremerhaven, Germany
[2]Deutsches Zentrum für Luft- und Raumfahrt (DLR), Institut für Physik der Atmosphäre, Oberpfaffenhofen, 82234 Weßling, Germany
[3]Institut für Umweltphysik, University Heidelberg, Im Neuenheimer Feld 229, 69120 Heidelberg, Germany
*now at: Forschungszentrum Jülich GmbH, Institut für Energie- und Klimaforschung IEK-8: Troposphäre, 52425 Jülich, Germany

*Correspondence to:* R. Weller (rolf.weller@awi.de)

**Abstract.** Continuous black carbon (BC) observations were conducted from 1999 through 2009 by an Aethalometer (AE10) and from 2006 through 2011 by a Multi-Angle Absorption Photometer (MAAP) at Neumayer Station (NM) under stringent contamination control. Considering the respective observation period, BC concentrations measured by the MAAP were somewhat higher (median $\pm$ standard deviation: $2.1 \pm 2.0 \, \text{ng m}^{-3}$) compared to the AE10 results ($1.6 \pm 2.1 \, \text{ng m}^{-3}$). Neither for the AE10 nor for the MAAP data set a significant long-term trend could be detected. Consistently a pronounced seasonality was observed with both instruments showing a primary annual maximum between October and November and a minimum in April with a maximum/minimum ratio of $4.5/1.6 = 3.8$ and $2.7/0.64 = 4.2$ for the MAAP and AE10 data, respectively. Occasionally a secondary summer maximum in January/February was visible. With the aim to assess the impact of BC on optical properties of the aerosol at NM, we evaluated the BC data along with particle scattering coefficients measured by an integrating nephelometer. We found the mean single scattering albedo of $\omega_{550} = 0.992 \pm 0.0090$ (median: 0.994) at a wavelength of 550 nm with a range of values from 0.95 to 1.0.

## 1 Introduction

Among sulfate, mineral dust, and water soluble inorganic compounds (e.g. ionic compounds originating mainly from sea salt aerosol production as well as ammonia and nitrate), carbonaceous aerosols represent one of the major fractions of tropospheric aerosols (Ramanathan et al., 2001; Forster et al., 2007). Aerosol particles influence the global radiation balance directly and can additionally act as condensation nuclei for cloud droplets, which in turn affect climate (Haywood and Boucher, 2000; Hatzianastassiou et al., 2004). Extinction of solar radiation in the visible and near UV range by carbonaceous aerosols is dominated by absorption and not by scattering (Horvath, 1993; Bond and Bergstrom, 2006). Actually, apart from carbonaceous aerosol, only mineral dust shows significant absorption of visible light, caused by variable amounts of haematite ($Fe_2O_3$) which result in a considerable imaginary part of the complex refractive index in the blue and green spectral range (Clarke and Charlson, 1985; Petzold et al., 2009).

There exist various terminologies for the light-absorbing fraction of the carbonaceous aerosol (Bond and Bergstrom, 2006; Andreae and Gelencsér, 2006). Despite the ambiguous definition, we refer to the term black carbon which is defined as combustion-produced black particulate carbon having a graphitic-like microstructure (Novakov, 1984) because it is widely used in climate research. However, it has to be noted that precisely speaking we refer to equivalent BC because for all applied optical methods the principal measure is light absorption which then is converted into mass of light-absorbing BC by applying a mass-specific absorption coefficient (MAC); see e.g. Bond and Bergstrom (2006).

Black carbon is exclusively produced by combustion of fossil fuels or biomass (Cachier, 1995). The remaining and larger fraction of carbonaceous aerosol (about 70–90 %) consists of highly polymerized organic material, so-called organic carbon (OC), which mainly scatters solar radiation comparable to sulfate aerosols (Cachier, 1995). Recent model calculations assessing the influence of aerosols on the global radiation budget have shown that the radiative forcing of carbonaceous aerosols is contrary to all other aerosol species: While the latter, including the weak light absorbing mineral dust, provoke a net cooling and thus mitigate the impact of greenhouse gases, the radiative forcing of carbonaceous aerosols is mainly positive and consequently leads to an amplification of the greenhouse warming (Andreae, 2001; Hatzianastassiou et al., 2004; Hansen et al., 2005; Seinfeld, 2008; Mahowald et al., 2011). Hansen et al. (2005), however, showed that for carbonaceous aerosol the situation is somewhat complicated by the fact, that in global models fossil fuel BC + OC clearly provoke positive forcing, while for biomass burning BC + OC a negative forcing dominates. The reliability of the amount of forcing on a global scale and especially its regional dependence is largely determined by the accuracy of the modelled aerosol distribution which finally relies on the availability of global BC emission and concentration data. While the northern hemisphere is clearly dominated by industrial BC emissions, within the southern hemisphere BC emissions by biomass burning (natural, fire clearing and household) are decisive (Koch et al., 2005). Especially in Polar Regions the positive forcing of absorbing aerosol should be most striking due to inherently high surface albedo caused by snow, sea ice and glacial ice coverage (Warren and Clarke, 1990; Forster et al., 2007). Indeed, there are some indications that BC and its deposition on snow may have substantially contributed to the rapid warming entailed by sea ice loss in the Arctic (Hansen et al., 2005).

Concerning the global distribution of carbonaceous aerosols, there is a major lack of observations at high southern latitudes, most notably Antarctica. This is especially disturbing, considering the recent enormous boost in the mainly ship borne Antarctic tourism activities during austral summer (Shirsat and Graf, 2009; Graf et al., 2010). Previous measurements indicate a geographical gradient of atmospheric BC concentrations from South Pole to Southern Ocean with minimum BC concentrations at South Pole (around $0.65 \, \mathrm{ng \, m^{-3}}$, Bodhaine, 1995), slightly increasing to coastal Antarctic sites (around $1 \, \mathrm{ng \, m^{-3}}$ at Halley, Wolff and Cachier, 1998), but significantly higher at the Antarctic Peninsula ($8.3 \, \mathrm{ng \, m^{-3}}$, Pereira et al., 2006). Neither of these investigations provided a trend estimate for BC concentrations, mainly due to short observation periods. Very recently, a study on global decadal trends of aerosol optical properties revealed no significant long term trend for BC concentrations observed at Neumayer (Collaud Coen et al., 2012). Individual ice core studies showed highly decadal scale BC deposition variability during the last 150 yr, but an anthropogenic impact could not be assessed (Bisiaux et al., 2012a and b).

In this paper we present an analysis of our BC concentration record from the German Antarctic Station Neumayer (NM), starting in 1999 and comprising now 13 yr of continuous measurements. First of all, this analysis will comprise a reanalysis of the BC long term trend, now including our observations made by a Multi-Angle Absorption Photometer (MAAP) started in March 2006, which was not included in the trend analysis mentioned above (Collaud Coen et al., 2012). In addition we will primarily focus on seasonal aspects and finally on the impact of BC on the bulk optical properties of the aerosol at NM.

## 2 Experimental techniques and data evaluation methods

### 2.1 Site description

BC measurements were conducted at the Air Chemistry Observatory, Neumayer Station (70°39′ S, 8°15′ W, http://www.awi.de/en/go/air_chemistry_observatory) which participates in the Global Atmosphere Watch (GAW) programme. A detailed description of the measuring site, meteorological conditions, contamination free sampling was already presented and we refer here to Wagenbach et al. (1988), König-Langlo et al. (1998) and Weller et al. (2008). Because in particular BC measurements are highly prone to the impact of local contamination, we will respond to this crucial aspect here again. First of all, the Air Chemistry Observatory is situated in the clean air district approximately 1.5 km south of NM and power supply is provided by cable from the main station. Due to the fact that northerly wind directions are very rare, contamination from the base can be excluded for most of the time. Furthermore, contamination-free sampling is additionally controlled by the permanently recorded wind velocity, wind direction and by the condensation particle (CP) concentration. Contamination was indicated for each of the following criteria: Wind direction within a 330°–30° sector, wind velocity $< 2.0 \, \mathrm{m \, s^{-1}}$ and/or CP concentrations (measured by a TSI CPC 3022A particle counter) $> 2500 \, \mathrm{cm^{-3}}$ during summer, $> 800 \, \mathrm{cm^{-3}}$ during spring/autumn and $> 400 \, \mathrm{cm^{-3}}$ during winter. The CP threshold values were chosen based on our more than 25-yr long CP record from Neumayer, demonstrating that CP concentrations above the corresponding levels can usually be traced back to local pollution. In fact, only during such conditions, BC concentrations frequently showed suspicious spikes exceeding $100 \, \mathrm{ng \, m^{-3}}$ by far. In the end, about 2 % of data loss was actually caused by potential contamination according to the criteria mentioned previously.

## 2.2 Instrumentation and data evaluation methods

### 2.2.1 Aerosol absorption photometer

Black carbon measurements with aerosol absorption photometers are based on the optical attenuation method described in general by Hansen et al. (1982, 1984). In short, BC is collected by drawing ambient air through a filter. The transmission of light through the loaded filter is related to the transmission through a clean part of the filter material. Knowledge of the specific BC attenuation cross section on the filter in use ($Q_{BC}$) finally allows the calculation of BC concentrations. This approach requires that the main aerosol species absorbing visible light at the considered wavelength is actually BC. In fact only haematite ($Fe_2O_3$), naturally occurring as a minor compound in mineral dust, has a significant, but two orders of magnitude lower absorption cross section in the visible compared to BC (Clarke and Charlson, 1985). Recent studies on the wavelength-dependence of the light absorption by mineral dust demonstrated that cross-sensitivities of light absorption methods for BC measurement are relevant for the wavelength of 550 nm and shorter while they can be almost neglected for the red spectral region (Petzold et al., 2011). Considering the generally low mineral dust concentrations at NM, typically in the lower ng m$^{-3}$ range (Weller et al., 2008) and the operational wavelengths of the applied instruments (Aethalometer: around 800 nm; MAAP: 637 nm), this possible interference was neglected throughout this work.

At Neumayer BC concentrations were continuously monitored by a white light Aethalometer (Magee Scientific, type AE10) from 1999 through 2009. Apart from several problems concerning the relation of the measured absorption signal to actual BC concentrations (e.g. Weingartner et al., 2003; Collaud Coen et al., 2010), this instrument is well-established and was used worldwide for many years, including pristine Antarctic sites like South Pole (Bodhaine, 1995) and Halley (Wolff and Cachier, 1998). The AE10 accumulated the aerosol on a circular spot with an area determined to be $107 \pm 2$ mm$^2$. We employed high volume filters (Pallflex, type T60A20; material: Pure borosilicate glass fibers with moisture-resistant tetrafluoroethylene coating) with a flow rate of 2.37 m$^3$ h$^{-1}$. The detection limit (DL), i.e. three times the standard deviation (std) of the noise level was derived from the output signals when the Aethalometer was operated with zero air (ambient air passed through two quartz filters in series or one HEPA filter). Referring to the original temporal resolution (sampling period t) of 4 h the DL was around 5 ng m$^{-3}$ which corresponds to a DL of around 10 ng m$^{-3}$ for 1 h resolution (assuming a $1/\sqrt{t}$ dependence, supported by the fact that the noise signal was normally distributed). This raw data set was finally combined into daily means and medians. The manufacturer notes that under normal performance the instrument should be able to detect approximately 1 ng BC, but recommend a more conservative value of 5 ng

BC. This would result in a nominal DL of 0.6 ng m$^{-3}$ BC for a 4 h sampling interval, which appeared highly optimistic as already stated before by Nyeki et al. (1998). In addition it was found that the sensitivity of the method decreased when the BC loading on the filter becomes high. We found that the noise level slightly increased when the sample filter was preloaded with black carbon, e.g. a test loading of 1850 ng to 3350 ng BC deteriorated the detection limit by a factor of 1.1 to 1.4. To prevent an appreciable loss in sensitivity, we changed the filters if the optical attenuation $-\ln(I/I_0)$ (where $I$ and $I_0$ are the transmitted light intensities for an exposed and a blank portion of the filter) exceeded a value 0.22, corresponding to a BC quantity of 1570 ng. More problematic is the impact of increasing light scattering with increasing aerosol load of the filter, biasing the results to the higher end. Up to now there exists no generally accepted procedure to correct this interference (Collaud Coen et al., 2010; Müller et al., 2011). The reduction of optical path length in the filter with increasing load was considered by the so-called Weingartner correction (Weingartner et al., 2003; Müller et al., 2011) and a more recent correction by Collaud Coen et al. (2010; equation 13 therein). Both corrections depend on the single scattering albedo of the aerosol $\omega_0$, which was derived from nephelometer data combined with MAAP results (see below) in order to avoid circular reasoning. It turns out that these corrections were well below 1 % throughout and thus negligible in case of the NM measurements. Due to the fact that such a procedure was impossible before March 2006 (start of the MAAP measurements) we finally refrain from correcting the AE10 data.

Since March 2006 ongoing a more sophisticated MAAP (Model 5012, Thermo Electron Corp.) is in operation, especially circumventing successfully the stray light problem (Petzold and Schönlinner, 2004; Petzold et al., 2005). Aerosol was sampled on a glass filter tape (Schleicher and Schüll, type GF 10) at an inlet air flow of 1.0 m$^3$ h$^{-1}$. The filter tape was automatically moved forward when the transmission exceeded 20 %. The measured absorption refers to a wavelength of 637 nm (Müller et al., 2011). Raw data were originally sampled in one minute resolution. Finally hourly, as well as daily means and medians were extracted. Hourly averaged MAAP data went rarely to negative values (12.8 % of the data), whereas for the AE10, even the 4-h samples fluctuated around zero (26.9 % of the data). A similar behavior was observed during side-by-side operations of an Aethalometer and a MAAP at the Jungfraujoch observatory (Petzold and Schönlinner, 2004). These fluctuations indicate BC values close to or below the DL. Consequently, we generally did not remove negative values because such a procedure would bias the data to higher values. Daily median MAAP data never showed negative values, while still about 8 % of the AE10 values were below zero (range between $-1.0$ and 0 ng m$^{-3}$). Thus all further data evaluation was based on daily medians. We found a MAAP detection limit of around 6.3 ng m$^{-3}$ BC for hourly resolution, which

appeared somewhat better than the DL of $< 20\,\text{ng m}^{-3}$ for 30 min means reported in the original paper (Petzold and Schönlinner, 2004). Extending the averaging period to 24 h with a flow of $1.0\,\text{m}^3\,\text{h}^{-1}$ would result in a reduced DL of $0.25\,\text{ng m}^{-3}$.

The accuracy of BC measurements by aerosol absorption photometers depends on the validity of the specific BC attenuation cross section ($Q_{BC}$) which is dependent on the used filter material. $Q_{BC}$ is $14\,\text{m}^2\,\text{g}^{-1}$ for the AE10 operated with Pallfex filters (provided by the manufacturer; note that a factor of $19\,\text{m}^2\,\text{g}^{-1}$ was recommended for often used quartz filters. Both values include filter artefacts). According to Müller et al. (2011) a $Q_{BC}$ of $6.6\,\text{m}^2\,\text{g}^{-1}$ was used for the MAAP. However, it should be mentioned that values in the range from $5\,\text{m}^2\,\text{g}^{-1}$ up to $20\,\text{m}^2\,\text{g}^{-1}$ have been found in ambient samples (Liousse et al., 1993; Petzold et al., 1997). Apart from this, it has to be stated very clearly that $Q_{BC}$ is different from MAC for which a recent review recommend a value of $7.5 \pm 1.2\,\text{m}^2\,\text{g}^{-1}$ at a wavelength of 550 nm (Bond and Bergstrom, 2006). According to Bodhaine et al. (1995) we suppose that the method dependent $Q_{BC}$ vary proportional to physically defined MAC so the ratio might be expected to be fairly constant. Both instruments operated at NM were not absolutely calibrated on-site, hence a stringent accuracy designation could not be given. As a reasonable assumption we refer to the DL as a crude measure for accuracy. For daily averaged BC concentration, the accuracy for the AE10 and MAAP would thus correspond to $\pm 2.1\,\text{ng m}^{-3}$ and $\pm 1.3\,\text{ng m}^{-3}$, respectively. We emphasize that this estimate includes uncertainties concerning light transmission, flow rate, and BC deposition area on the filter but not uncertainties arising from the actual specific absorption coefficients $Q_{BC}$ and MAC. Due to the inferior quality of the AE10 data, we considered the MAAP results as more reliable and focus for the main part of our evaluation and reasoning on this data set. Nevertheless we are confident that also the AE10 data represent a consistent and valuable BC time series.

The AE10 and the MAAP were both connected to the central inlet duct of the observatory, a ventilated electro-polished stainless steel inlet stack (total height about 8 m above the snow surface) with a 50 % aerodynamic cut-off diameter around 7–10 µm at wind velocities between 4–10 m s$^{-1}$ (determined with an aerodynamic particle sizer TSI, type APS 3321). From the stack to the MAAP and AE10 we used silicone conductive tubes each with a length of around 50 cm, hence the inlet characteristic of both instruments were virtually identical.

Apart from the contamination screening procedure an additional data selection was necessary for the AE10: During stormy weather conditions (typically at wind velocities above 20 m s$^{-1}$), sometimes extraordinarily noisy signal output occurred, possibly caused by sea salt deposition on the filter. In such cases spikes in the original data set typically exceeding some 100 ng m$^{-3}$ were immediately followed (i.e. in the subsequent measuring interval) by comparably large spikes in the opposite direction. Such cases could be easily identified and were treated as fake signals and discarded throughout, because an evaluation was not meaningful.

### 2.2.2 Auxiliary measurements

In order to assess the impact of BC on the optical properties of the aerosol, BC concentrations have to be converted to particle absorption coefficients $\sigma_{ap}(\lambda)$ (unit: $1\,\text{Mm}^{-1} = 10^6\,\text{m}^{-1}$) by using the specific BC absorption on the filter material ($Q_{BC}$). Note that although light attenuation caused by aerosol deposition on the filter was primarily measured, the recorded output signals finally correspond to BC concentrations internally calculated by using the respecting $Q_{BC}$. This part of the evaluation was restricted to the MAAP data, because the operating wavelength and spectral sensitivity of the AE10 detection optic is ill defined (Weingartner et al., 2003). For the MAAP, we relied on the operative wavelength of 637 nm. In addition to BC data, we employed particle scattering coefficients measured with an integrating three wavelength nephelometer (TSI, model 3563), in operation since 2001, and snow surface albedo measurements $R_s$, started in 1982. A thorough discussion of these time series is a matter of its own and beyond the scope of this paper. Hence we merely present the time series of these parameters in the Supplement (Figs. S.1 to S.3).

Operation of the nephelometer and data evaluation have previously been described in detail by Weller and Lampert (2008). In short, particle scattering $\sigma_{sp}(\lambda)$ and hemispheric back-scattering $\sigma_{bsp}(\lambda)$ coefficients were originally determined in 10 min averages at the wavelengths 450 nm, 550 nm, and 700 nm. After correction for non-Lambertian illumination and truncation errors (according to Anderson and Ogren, 1998) hourly averages were extracted and used for further evaluation. The hemispheric back-scattering fraction $b_\lambda$ was calculated according to:

$$b_\lambda = \sigma_{bsp}(\lambda)/\sigma_{sp}(\lambda) \tag{1}$$

Surface albedo measurements started at Georg von Neumayer, GvN in 1982. In the meanwhile these measurements are embedded within a wider observation program and are part of the Baseline Solar Radiation Network (BSRN, Ohmura et al., 1998, http://www.bsrn.awi.de/en/home/bsrn/) since March 1992. Snow surface albedo was determined by two identical pyranometers of the type CM11, CM22, or CMP22, respectively (Kipp&Zonen, The Netherlands), integrating global solar and reflected radiation within a spectral range from 305 nm to 2800 nm. The temporal resolution of the original data was 10, 5, and 1 min for the CM11, CM22, and CMP22, respectively, but for our purpose exclusively daily means were used. Surface albedo measurements were critical at very low solar radiation (large solar zenith angles) and frequently exhibited strong diurnal cycles due to snow ripples (sastruga) reflections especially under clear
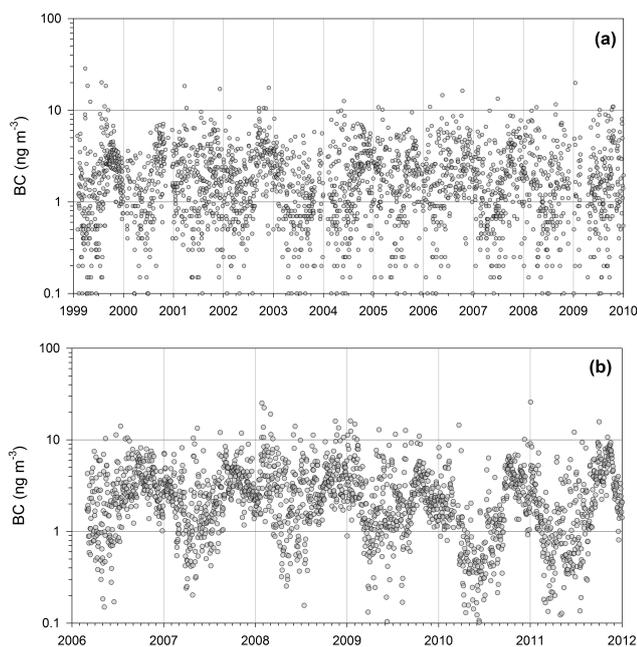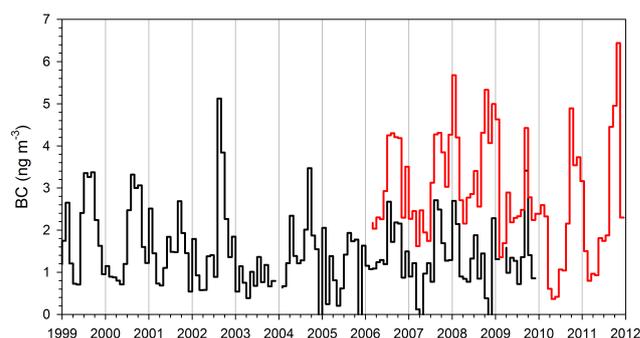
**Fig. 1.** BC time series, based on daily medians, measured by the Magee Scientific AE10 Aethalometer **(a)** and by the MAAP **(b)**. Vertical grey lines mark the turn of the year.

sky conditions (Pirazzini, 2004; Wuttke et al., 2006). Such impacts are obviated by using daily means of radiation data and additionally excluding all global radiation values below a daily mean of $10\,\mathrm{W\,m^{-2}}$.

## 3 Data presentation

Figure 1a shows the BC time series measured by the AE10, while in Fig. 1b the results from the MAAP are presented. Individual data points refer to daily medians, which could be described by a log-normal distribution (see Supplement S.4). Figure 2 shows the monthly means of both time series together. Obviously the AE10 data with an overall median (mean) of $1.60\,\mathrm{ng\,m^{-3}}$ ($2.20\,\mathrm{ng\,m^{-3}}$) for the whole period (1999 through 2009) and $1.55\,\mathrm{ng\,m^{-3}}$ ($2.23\,\mathrm{ng\,m^{-3}}$) regarding the overlapping period with the MAAP (March 2006 through 2009) appeared somewhat lower compared to the MAAP data with a long-term median of $2.14\,\mathrm{ng\,m^{-3}}$ ($2.60\,\mathrm{ng\,m^{-3}}$) and $2.34\,\mathrm{ng\,m^{-3}}$ ($2.77\,\mathrm{ng\,m^{-3}}$) for the overlapping period.

A linear reduced major axis (RMA) regression of $BC_{aeth}$ vs. $BC_{MAAP}$ (daily medians) resulted in a slope of $0.82 \pm 0.03$ with an intercept of $0.86 \pm 0.1$ ($r^2 = 0.19$, $n = 928$; Fig. 3). Note that a RMA regression based on weekly medians resulted in a comparable poor correlation (slope $= 0.96 \pm 0.07$, intercept $= -0.53 \pm 0.36$, $r^2 = 0.26$), potentially related to the fact that both instruments operate close to their lower limit of detection which caused very noisy data.



**Fig. 2.** Complete BC time series based on monthly means. The black and red line represents the data measured by the AE10 and the MAAP, respectively.
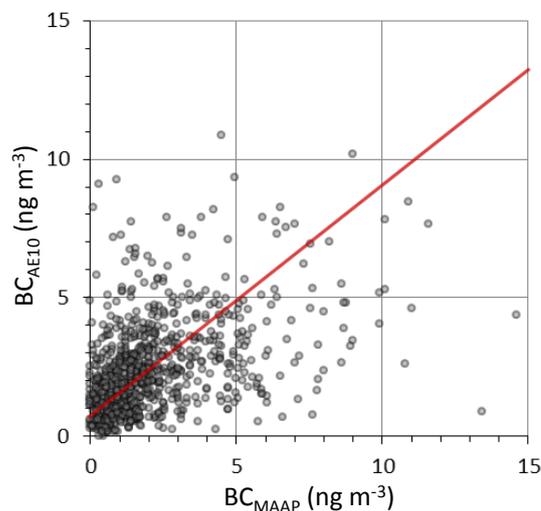


**Fig. 3.** RMA regression of BC concentrations (daily medians) measured by the AE10 and the MAAP. Slope $= 0.82 \pm 0.03$, intercept $= 0.86 \pm 0.1$, $r^2 = 0.19$, $n = 928$).

Due to the poor correlation between both data sets, a reliable homogenization emerged unsuccessful and we preferred a separate trend analysis on each time series. A nonparametric rank-order Mann Kendall test with Sen's slope trend analysis (Hirsch et al., 1982) revealed that for the individual segments measured by the MAAP or AE10 no significant overall trend could be detected, in accordance with the trend analysis already presented for the AE10 time series (Collaud Coen et al., 2012; note that therein a statistically significant but marginal negative trend of $-0.01\,\mathrm{ng\,m^{-3}\,yr^{-1}}$ was found and finally discarded due to high percentage of negative values). A monthly resolved analysis showed significant ($p < 0.05$) but opposite trends for the months June and August ($-0.51\,\mathrm{ng\,m^{-3}\,yr^{-1}}$ and $+0.14\,\mathrm{ng\,m^{-3}\,yr^{-1}}$, respectively) for the MAAP data. As for the AE10 time series, slight negative trends for the months November and December ($-0.09\,\mathrm{ng\,m^{-3}\,yr^{-1}}$ and $-0.11\,\mathrm{ng\,m^{-3}\,yr^{-1}}$, respectively) could be detected.
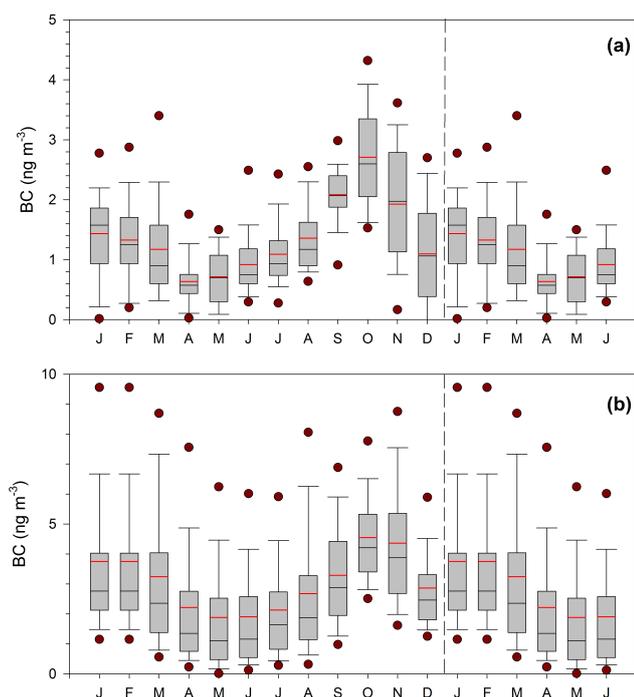
**Fig. 4.** Box plots of the mean seasonality of BC concentrations based on daily medians: Results measured by the AE10 for the years 1999–2009 **(a)** and by the MAAP for the period 2006–2011. Lines in the middle of the boxes represent sample medians (mean: red line), lower and upper lines of the boxes are the 25th and 75th percentiles, whiskers indicate the 10th and 90th percentiles, dots 5th and 95th percentiles. The graph comprises 18 months starting from January to show the summer maximum without cease.

Apart from the obvious discrepancy of both data sets and the weak correlation between them, the mean seasonality was in agreement (Fig. 4), indicating that the AE10 data reliably described the annual BC cycle at NM. With both instruments a primary annual maximum between October and November and a minimum in April was visible with a maximum/minimum ratio of $4.5/1.6 = 3.8$ and $2.7/0.64 = 4.2$ for the MAAP and AE10 data, respectively. A closer inspection revealed that BC concentrations measured by the MAAP appeared also relatively high for the months January and February a feature which was not reflected by the AE10 data (Fig. 4). It seems that this double maximum was not an artifact provoked by the averaging process but was also present during the individual austral summers 2007/2008, 2008/2009 and 2009/2010 (Fig. 2).

## 4   Discussion

### 4.1   Long term trend

A discussion of trend and seasonality requires that the specific BC attenuation cross section ($Q_{BC}$) was all about the same throughout the measuring period. This assumption ap-

peared reasonable considering the fact that BC from biomass burning is well aged (long range transport time to coastal Antarctica is typically > 5 days according to Stohl and Sodemann, 2010) and the physico-chemical state of BC aerosol should be consistent. Indeed, Liousse et al. (1993) and Petzold et al. (1997) found $Q_{BC}$ to be constant in a given atmospheric environment. Furthermore we argue that the impact of local BC was generally negligible, except from some few sporadic events (see below). This conclusion was supported by the annual cycle of the observed BC concentrations showing a broad maximum around October/November (Fig. 4). In contrast, local BC pollution at NM should have a striking maximum starting in the middle of December through the end of February. Supply and removal activities of the station happened within this time frame each year, associated with heavy freight traffic. Nevertheless there are some indications pointing to a minor but not negligible impact of local contamination. These are occasional secondary BC maxima in the MAAP data around January and apparently high BC concentrations observed from November 2007 through February 2009 (Figs. 1 and 2), the period when the new construction of Neumayer III Station was afoot.

Although ice core records indicate a growing BC deposition in Antarctica (Bisiaux et al., 2012a and b), our results revealed a virtually constant long-term atmospheric BC level around $2 \, \text{ng m}^{-3}$ for the MAAP and $1.55 \, \text{ng m}^{-3}$ for the AE10 time series. Up to now no atmospheric BC trend analyses from other Antarctic sites are available, but BC concentrations at NM were comparable to previous atmospheric measurements from Halley (AE10 record, 1992–1995) with a mean around $1 \, \text{ng m}^{-3}$, but definitely lower than the annual mean BC concentrations of $8.3 \, \text{ng m}^{-3}$ observed with an AE9 in 1993, 1997, and 1998 on King George Island (Antarctic Peninsula) (Table 1). Chaubey et al. (2010) reported outstanding high BC concentrations during austral summer 2008/2009 from the coastal sites Maitri ($75 \pm 33 \, \text{ng m}^{-3}$) and Larsemann Hills ($13 \pm 4 \, \text{ng m}^{-3}$) measured with a Magee Scientific type AE41 aethalometer. At least for Maitri, a considerable impact of local pollution by human activities has to be considered (Chaubey et al., 2010). We conclude that BC concentrations between $1 \, \text{ng m}^{-3}$ and $2 \, \text{ng m}^{-3}$ can be regarded representative for coastal Antarctica except the northern parts of the Antarctic Peninsula (King George Island). Lowest BC concentrations ($0.65 \, \text{ng m}^{-3}$ measured with a Magee Scientific aethalometer, type not specified but most probably an AE10; Bodhaine 1995) were found at South Pole, a site which may be representative for the Antarctic Plateau. Figure 5 may serve as simplified survey of this geographical BC concentration gradient. Based on our data, there is up to now no conclusive evidence of significantly enhanced atmospheric BC pollution caused by increasing shipping activities (mostly tourism) in the South Atlantic peaking between December and March (Shirsat and Graf, 2009). Note, however, that Antarctic tourism is up to now mainly focused on the marine

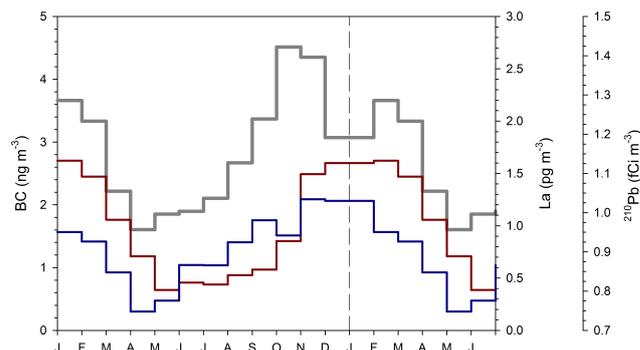**Table 1.** BC concentration measured at different Antarctic sites.

| site | geographical position | BC concentration | reference |
|------|----------------------|------------------|-----------|
| South Pole | 90° S | 0.65 ng m$^{-3}$ (annual mean) | Bodhaine (1995) |
| Halley | 75°35′ S, 26°14′ W | 1.0 ng m$^{-3}$ (annual mean) | Wolff and Cachier (1998) |
| Neumayer | 70°39′ S, 08°15′ W | 2.6 ng m$^{-3}$ (annual mean) | this study |
| Ferraz, King George Island | 62°05′ S, 58°23′ W | 8.3 ng m$^{-3}$ (annual mean) | Pereira et al. (2006) |
| Maitri | 70°46′ S 11°44′ E | 75 ng m$^{-3}$ (summer) | Chaubey et al. (2010) |
| Larsemann Hills | 69°44′ S, 76°11′ E | 13 ng m$^{-3}$ (summer) | Chaubey et al. (2010) |
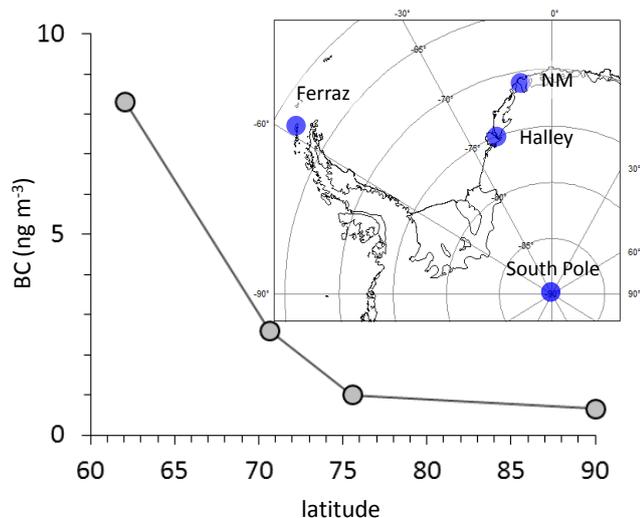


**Fig. 5.** Spatial BC concentration gradient in Antarctica. Only sites from which annual mean values were available are shown; references can be found in Table 1.



**Fig. 6.** Seasonality (monthly means) of typical terrestrial tracers measured at NM: BC (grey line, measured by the MAAP), the rare earth element La (red line), a tracer for mineral dust, and $^{210}$Pb (blue line) a progeny of the terrigenous noble gas $^{222}$Rn. The graph comprises 18 months starting from January to show the seasonal maxima without cease.

## 4.2 Seasonality and dependence on general weather situation

Black carbon concentrations at NM showed a broad annual maximum around October/November, consistent in relative amplitude and phase with measurements conducted at Halley (Wolff and Cachier, 1998), South Pole (Bodhaine 1995), and Antarctic Peninsula (Pereira et al., 2006). Biomass burning in Africa, South America and Australia is the main BC source in the southern hemisphere (van der Werf et al., 2006 and 2008). Given the fact that large scale meridional transport was mainly provoked by cyclonic activity (Pereira et al., 2006; Fiebig et al., 2009; Hara et al., 2010), we expect higher BC concentrations at NM during passing of low pressure systems which was generally characterized by strong easterly winds at NM. In fact BC concentrations were significantly higher (2.85 ng m$^{-3}$) during storms (wind velocity > 15 m s$^{-1}$ and wind direction between 0° and 120°) compared to the annual median (2.14 ng m$^{-3}$) or to 1.64 ng m$^{-3}$

encountered during calm weather conditions (wind velocity < 7 m s$^{-1}$, wind direction between 120° and 360°). Another potential transport mechanism, in particular during polar night, could be subsidence of middle and upper tropospheric air above central Antarctica associated with horizontal advection by katabatic wind to coastal Antarctica (James, 1989; Van de Berg et al., 2007). Actually, we could not find any indications that southerly winds (indicative for downslope or katabatic flow, König-Langlo et al., 1998) were associated with enhanced BC concentrations at Neumayer (the same is true for mineral dust tracers) and the seasonality of the mentioned tracers is in conflict with air mass transport from the Antarctic Plateau by catabatic outflow.

Results from Pereira et al. (2006) and Fiebig et al. (2009) indicate that South America is the main BC source region for the Weddell Sea and Dronning Maud Land region. There, biomass burning typically peaks in late winter/early spring (September–October), i.e. around 1–2 months earlier compared to BC concentration maxima typically observed in Antarctica (van der Werf et al., 2006 and 2008). The dominant biomass burning region in South America is Amazonia, extending to northern Argentina around 45° S (van der Werf et al., 2006; see also http://rapidfire.sci.gsfc.nasa.gov/firemaps/). Apart from BC, the dominant source region for

R. Weller et al.: Characterization of long-term and seasonal variations of BC

mineral dust aerosol entry in Antarctica is also South America (Smith et al., 2003). Figure 6 presents the mean annual cycle of BC in combination with the rare earth element La (a tracer for mineral dust; data from Weller et al. 2008) and a further terrigenous tracer, $^{210}$Pb (data from Elsässer et al., 2011) all observed at NM. Given that for these three tracers South America was the main source region, a comparison of their annual cycle observed at NM may give some insight on the interplay of source variability (including vertical exchange processes with the free troposphere), large scale meridional transport efficiency (including depositional loss en route), and boundary layer inversion strength at NM (affecting downward mixing) in determining the concentrations finally measured at NM. For $^{210}$Pb and the mineral dust tracer La a broad summer maximum was evident, slightly shifted to January/February for La (Fig. 6). The main seasonal maximum of BC was about 3 months early. For biomass burning a strong seasonality and patchy, sporadic occurrence is evident (van der Werf et al., 2006 and 2008). While also mineral dust sources are generally patchy and sporadic, their seasonality in South America is somewhat ambiguous, though a broad maximum between October and March is discernible (Gaiero et al., 2003). Atmospheric mixing height should also be at maximum during summer supporting vertical exchange of air masses. Deposition efficiency should be larger for the supra-micrometer mineral dust (Sanak et al., 1981) compared to BC, a typical sub-micrometer aerosol species (Seinfeld and Pandis, 2006a; Adachi and Buseck, 2008). As for $^{210}$Pb, a decay product of the noble gas $^{222}$Rn which is continuously emitted from soil, the annual cycle of the continental source strength is relatively weak. Note that at NM, oceanic emissions peaking after the retreat of the sea ice in late summer might add to the local atmospheric $^{222}$Rn inventory during that time (Elsässer et al., 2011). The effect on the $^{210}$Pb seasonality is, however, not clear yet. Long range transport of $^{210}$Pb and maybe also of BC should be more efficient compared to mineral dust due to the smaller atmospheric residence time of the latter. Large scale meridional transport towards Antarctica, most probably via the free troposphere should be most favorable after decay of the polar vortex in summer (Genthon, 1992; Krinner and Genthon, 2003; Stohl and Sodemann, 2010). This is also the time when surface inversion strength at NM was at minimum (Elsässer et al., 2011), facilitating down mixing from the free troposphere into the planetary boundary layer. Therefore the seasonality of virtually all processes relevant for mineral dust generation and transport as well as $^{210}$Pb transport to NM were in phase and consistent with the observed annual maximum (Weller et al., 2008; Elsässer et al., 2011). On the other hand, the annual BC cycle observed at NM was presumably shaped by a convolution of the more pronounced and earlier biomass burning maximum in September/October and the seasonal maximum of large scale meridional transport efficiency during austral summer. The impact of biomass burning seasonality appeared considerable if not dominant, hence observed BC concentrations apparently reflect essentially the variability of biomass burning in South America.

## 4.3 Impact on aerosol optical properties

In order to assess the impact of BC on optical aerosol properties at NM, we calculated the single scattering albedo ($\omega_{550}$) as well as the critical single scattering albedo ($\omega_{\mathrm{crit}}$) for the wavelength $\lambda = 550$ nm (Seinfeld and Pandis, 2006b):

$$\omega_{550} = \sigma_{\mathrm{sp}}(550)/(\sigma_{\mathrm{sp}}(550) + \sigma_{\mathrm{ap}}(550)) \tag{2}$$

$$\omega_{\mathrm{crit}} = 2R_{\mathrm{s}}/(2R_{\mathrm{s}} + b_{550}(1 + R_{\mathrm{s}})^2) \tag{3}$$

The critical single scattering albedo $\omega_{\mathrm{crit}}$ provides a crude estimate whether aerosol forcing was negative ($\omega_{\mathrm{crit}} < \omega_{550}$) or positive ($\omega_{\mathrm{crit}} > \omega_{550}$) (Seinfeld and Pandis, 2006b). To this end we made use of aerosol light scattering coefficient, hemispheric backscattering fraction $b_{550}$ at 550 nm, and surface albedo ($R_{\mathrm{s}}$) values from our continuous nephelometer and radiation measurements, respectively. BC concentrations reported by the MAAP were re-converted to aerosol absorption coefficients at 550 nm ($\sigma_{\mathrm{ap}}(550)$) using the firmware coefficient of $6.6\,\mathrm{m}^2\,\mathrm{g}^{-1}$ at $\lambda = 637$ nm and extrapolated to $\lambda = 550$ nm accepting a $\lambda^{-1}$ dependence of $\sigma_{\mathrm{ap}}(\lambda)$ (Horvath, 1993; Schnaiter et al., 2003). Note that for $R_{\mathrm{s}}$ only broadband values (305 nm to 2800 nm) were available. Spectral snow surface albedo measurements at NM indicate a maximum close to 1.0 at 500 nm, decreasing to around 0.95 at 300 nm and between 0.45 and 0.75 at 1000 nm (Wuttke et al., 2006). As already mentioned in Section 2.2.1, the time series of the respective parameters $\sigma_{\mathrm{sp}}(550)$, $\sigma_{\mathrm{bsp}}(550)$, and $R_{\mathrm{s}}$ are presented in the Supplement (Figs. S.1 to S.3). In short, the long-term mean values and standard deviations were: $\sigma_{\mathrm{sp}}(550) = 4.37 \pm 5.8\,\mathrm{Mm}^{-1}$ (range: $0.1\,\mathrm{Mm}^{-1}$ to $59\,\mathrm{Mm}^{-1}$), $\sigma_{\mathrm{bsp}}(550) = 0.62 \pm 0.71\,\mathrm{Mm}^{-1}$ (range: $0.1\,\mathrm{Mm}^{-1}$ to $15.4\,\mathrm{Mm}^{-1}$), and $R_{\mathrm{s}} = 0.857 \pm 0.053$ (range: 0.51 to 1.0). In addition, a trend analysis of aerosol optical properties by nephelometer measurements at NM can be found in Collaud Coen et al. (2012).

The calculated daily mean values for $\omega_{550}$ and $\omega_{\mathrm{crit}}$ are presented in Fig. 7. In addition Fig. 8 may serve as an overview for the dependence of $\omega_{\mathrm{crit}}$ on $R_{\mathrm{s}}$ and hemispheric backscattering fraction $b_{550}$ values typical for NM as well as the range of the derived $\omega_{550}$ data. Based on this simple estimate, in most of the cases a net heating effect (positive forcing) of boundary layer aerosol at NM ($\omega_{550} < \omega_{\mathrm{crit}}$ in 69.5 % of the cases) was evident. Nevertheless, even under the highest measured $\sigma_{\mathrm{ap}}(550)$ (around $0.15\,\mathrm{Mm}^{-1}$, for daily medians) merely 0.015 % of the incident solar radiation at 550 nm would be absorbed in an atmospheric layer with an optical path length of 1 km. We conclude that any heating effect within the PBL was eventually negligible.
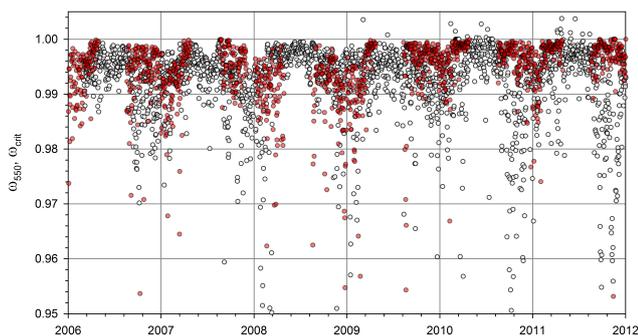
**Fig. 7.** Time series of the measured single scattering albedo at 550 nm, $\omega_{550}$ (black circles) along with the calculated critical single scattering albedo $\omega_{crit}$ (red circles). Note that $\omega_{crit}$ values were not available between end of April and early August of each year, because then solar radiation was below $10\,\mathrm{W\,m^{-2}}$ and $R_s$ could not be reliably determined.
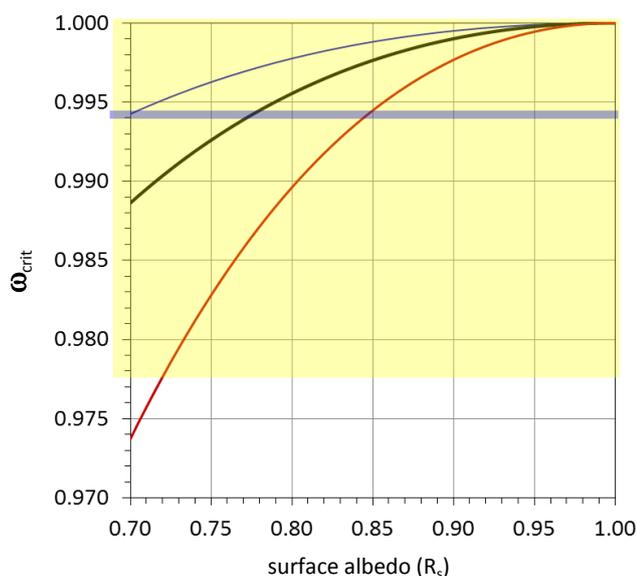


**Fig. 8.** Critical single scattering albedo $\omega_{crit}$ as a function of surface albedo $R_s$ typically found at NM; $\omega_{crit}$ is calculated for the mean (black line), maximum (blue line) and minimum (red line) hemispheric backscattering fraction measured by nephelometer at 550 nm. The yellow shaded region represents the 5 % to 95 % percentile range, the grey solid line the median of the measured $\omega_{550}$.

## 5 Conclusions

In light of the dramatically increasing human activities in Antarctica during the last few decades, the nearly constant annual median BC concentrations observed at NM from 1999 through 2011 appeared somewhat peculiar. Apart from the sporadic impact of local pollution, growing combustion derived emissions from ship borne activities in the Southern Ocean are, up to now, only of exiguous relevance for BC concentrations at NM. Large scale meridional transport of biomass-burning derived black carbon, preferentially

from South America, seems to determine the BC burden in Antarctica and caused a distinct and consistent spring / early summer concentration maximum. Nevertheless, without much doubt anthropogenic combustion derived emissions will perpetually grow around and within continental Antarctica. Hence there is a demand to continue observations with a view to document the impact of such activities on the Antarctic environment. In addition to atmospheric BC measurements such observations should especially include the critical role of BC deposition and its impact on surface albedo in Antarctica. Apart from the contribution of absorbing aerosol on the radiation balance of the Antarctic atmosphere at present, BC profiles measured in Antarctic ice cores could elucidate the potential increase since pre-industrial era and thus clearly constrain the respective human effect. Moreover, this effort might reveal the biomass burning history in ancient times including its relevance on climate forcing.

**Supplementary material related to this article is available online at: http://www.atmos-chem-phys.net/13/ 1579/2013/acp-13-1579-2013-supplement.pdf.**

## References

Adachi, K. and Buseck, P. R.: Internally mixed soot, sulfates, and organic matter in aerosol particles from Mexico City, Atmos. Chem. Phys., 8, 6469–6481, doi:10.5194/acp-8-6469-2008, 2008.

Anderson, T. L. and Ogren, J. A.: Determining aerosol radiative properties using the TSI 3563 integrating nephelometer, Aerosol Sci. Technol., 29, 57–69, 1998.

Andreae, M. O.: The dark side of aerosols, Nature, 409, 671–672, 2001.

Andreae, M. O. and Gelencsér, A.: Black carbon or brown carbon? The nature of light-absorbing carbonaceous aerosols, Atmos. Chem. Phys., 6, 3131–3148, doi:10.5194/acp-6-3131-2006, 2006.

Bisiaux, M. M., Edwards, R., McConnell, J. R., Albert, M. R., Anschütz, H., Neumann, T. A., Isaksson, E., and Penner, J. E.: Variability of black carbon deposition to the East Antarctic Plateau, 1800–2000 AD, Atmos. Chem. Phys., 12, 3799–3808, doi:10.5194/acp-12-3779-2012, 2012a.

Bisiaux, M. M., Edwards, R., McConnell, J. R., Curran, M. A. J., Van Ommen, T. D., Smith, A. M., Neumann, T. A., Pasteris, D. R., Penner, J. E., and Taylor, K.: Changes in black carbon deposition to Antarctica from two high-resolution ice core records, 1850–2000 AD, Atmos. Chem. Phys., 12, 4107–4115, doi:10.5194/acp-12-4107-2012, 2012b.

Bodhaine, B. A.: Aerosol absorption measurements at Barrow, Mauna Loa and the south pole, J. Geophys. Res., 100, 8967–8975, 1995.

Bond, T. C. and Bergstrom, R. W.: Light absorption by carbonaceous particles: an investigative review, Aerosol Sci. Technol., 40, 27–67, 2006.

Cachier, H.: Combustion carbonaceous aerosols in the atmosphere: Implications for ice-core studies, in: Ice Core Studies of Biogeochemical Cycles, Nato ASI Ser., edited by: Delmas, R., 30, 347–360, Springer-Verlag, New York, 1995.

Chaubey, J. P., Moorthy, K. K., Babu, S. S., Nair, V. S., and Tiwari, A.: Black carbon aerosol over coastal Antarctica and its scavenging by snow during the Southern Hemispheric summer, J.Geophys. Res., 115, D10210, doi:10.1029/2009JD013381, 2010.

Clarke, A. D. and Charlson, R. J.: Radiative properties of the background aerosol: Absorption component of extinction, Science, 229, 263–265, 1985.

Collaud Coen, M., Weingartner, E., Apituley, A., Ceburnis, D., Fierz-Schmidhauser, R., Flentje, H., Henzing, J. S., Jennings, S.G., Moerman, M., Petzold, A., Schmid, O., and Baltensperger, U.: Minimizing light absorption measurement artifacts of the Aethalometer: evaluation of five correction algorithms, Atmos. Meas. Tech., 3, 457–474, doi:10.5194/amt-3-457-2010, 2010.

Collaud Coen, M., Andrews, E., Asmi, A., Baltensperger, U., Bukowiecki, N., Day, D., Fiebig, M., Fjaeraa, A. M., Flentje, H., Hyvärinen, A., Jefferson, A., Jennings, S. G., Kouvarakis, G., Lihavainen, H., Lund Myhre, C., Malm, W. C., Mihapopoulos, N., Molenar, J. V., O'Dowd, C., Ogren, J. A., Schichtel, B. A., Sheridan, P., Virkkula, A., Weingartner, E., Weller, R., and Laj, P.: Aerosol decadal trends – Part 1: In-situ optical measurements at GAW and IMPROVE stations, Atmos. Chem. Phys., 13, 869–894, doi:10.5194/acp-13-869-2013, 2013.

Elsässer, C., Wagenbach, D, Weller, R., Auer, M., Wallner, A., and Christl, M.: Continuous 25-years aerosol records at coastal Antarctica: Part 2: variability of the radionuclides $^7$Be, $^{10}$Be and $^{210}$Pb, Tellus, 63B, 920–934, doi:10.1111/j.1600-0889.2011.00543.x, 2011.

Fiebig, M., Lunder, C. R., and Stohl, A.: Tracing biomass burning aerosol from South America to Troll Research Station, Antarctica, Geophys. Res. Lett., 36, L14815, doi:10.1029/2009GL038531, 2009.

Forster, P., Ramaswamy, V., Artaxo, P., Berntsen, T, Betts, R., Fahey, D. W., Haywood, J., Lean, J., Lowe, D. C., Myhre, G., Nganga, J., Prinn, R., Raga, G., Schulz, M., and Van Dorland, R.: Changes in Atmospheric Constituents and Radiative Forcing, in: Climate Change 2007: The Physical Science Basis. Contribution of Working Group I to the Fourth Assessment Report of the Intergovernmental Panel on Climate Change, edited by: Solomon, S., Qin, D., Manning, M., Chen, Z., Marquis, M., Averyt, K. B., Tignor, M., and Miller, H. L., 143–145, Cambridge University Press, Cambridge, UK and New York, NY, USA, 2007.

Gaiero, D. M., Probst, J.-L., Depetris, P. J., Bidart, S. M., and Leleyter, L.: Iron and other metals in Patagonian riverborne and windborne materials: Geochemical control and transport to the southern South Atlantic Ocean, Geochim, Cosmochim. Acta, 67, 3603–3623, 2003.

Genthon, C.: Simulations of desert dust and sea-salt aerosol in Antarctica with a general circulation model of the atmosphere, Tellus 44B, 371–389, 1992.

Graf, H.-F., Shirsat, S. V., Oppenheimer, C., Jarvis, M. J., Podzun, R., and Jacob, D.: Continental scale Antarctic deposition of sulphur and black carbon from anthropogenic and volcanic sources, Atmos. Chem. Phys. 10, 2457–2465, doi:10.5194/acp-10-2457-2010, 2010.

Hansen, A. D. A., Rosen, H., and Novakov, T.: Real-time measurement of the absorption coefficient of aerosol particles, Appl. Opt., 21, 3060–3062, 1982.

Hansen, A.D.A., Rosen, H., and Novakov, T.: The Aethalometer– An instrument for the real-time measurement of optical absorption by aerosol particles, Sci. Total Environ., 36, 191-196, 1984.

Hansen, J., Sato, M., Ruedy, R., Nazarenko, L, Lacis, A., Schmidt, G.A., Russel, G., Aleinov, I., Bauer, M., Bauer, S., Bell, N., Cairns, B., Canuto, V., Chandler, M., Cheng, Y., Del Genio, A., Faluvegi, G., Fleming, E., Friend, A., Hall, T., Jackman, C., Kelley, M., Kiang, N., Koch, D., Lean, J., Lerner, J., Lo, K., Menon, S., Miller, R., Minnis, P., Novakov, T., Oinas, V., Perlwitz, Ja., Perlwitz, Ju., Rind, D., Romanou, A., Shindell, D., Stone, P., Sun, S., Tausnev, N., Thresher, D., Wielicki, B., Wong, T., Yao, M., and Zhang, S.: Efficacy of climate forcings, J. Geophys. Res., 110, D18104, doi:10.1029/2005JD005776, 2005.

Hara, K., Osada, K., Yabuki, M., Hashida, G., Yamanouchi, T., Hayashi, M., Shiobara, M., Nishita, C., and Wada, M.: Haze episodes at Syowa Station, coastal Antarctica: Where did they come from?, J. Geophys. Res., 115, D14205, doi:10.1029/2009JD012582, 2010.

Haywood, J. and Boucher, O.: Estimates of the direct and indirect radiative forcing due to tropospheric aerosols: A review, Rev. Geophys., 38(4), 513-543, 2000.

Hatzianastassiou, N., Katsoulis, B., and Vardavas, I.: Global distribution of aerosol direct radiative forcing in the ultraviolet and visible arising under clear skies, Tellus, 56B, 51–71, 2004.

Hirsch, R. M., Slack, J. R., and Smith, R. A.: Techniques of trend analysis for monthly water quality data, Water Resour. Res. 18, 107–121, 1982.

Horvath, H.: Atmospheric light absorption – a review, Atmos. Environ., 27A, 293–317, 1993.

James, I. N.: The Antarctic drainage flow: implications for hemispheric flow on the Southern emisphere, Antarct. Sci., 1, 279–290, 1989.

Koch, D. and Hansen, J.: Distant origins of Arctic black carbon: A Goddard Institute for Space Studies ModelE experiment, J. Geophys. Res., 110, D04204, doi:10.1029/2004JD005296, 2005.

König-Langlo, G., King, J. C., and Pettré, P.: Climatology of the three coastal Antarctic stations Dumont d'Urville, Neumayer and Halley, J. Geophys. Res., 103, 10935–10946, 1998.

Krinner, G. and Genthon, C.: Tropospheric transport of continental tracers towards Antarctica under varying climatic conditions, Tellus 55B, 54–70, 2003.

Liousse, C., Cachier, H., and Jennings, S.G.: Optical and thermal measurements of black carbon aerosol content in different envi-

ronments: Variation of specific attenuation cross section, sigma ($\sigma$), Atmos. Environ., 27(A), 1203-1211, 1993.

Mahowald, N. M., Kloster, S., Engelstaedter, S., Moore, J. K., Mukhopadhyay, S., McConnell, J. R., Albani, S., Doney, S. C., Bhattacharya, A., Curran, M. A. J., Flanner, M. G., Hoffman, F. M., Lawrence, D. M., Lindsay, K., Mayewski, P. A., Neff, J., Rothenberg, D., Thomas, E., Thornton, P. E., and Zender, C. S.: Observed 20th century desert dust variability: impact on climate and biogeochemistry, Atmos. Chem. Phys., 10, 10875–10893, doi:10.5194/acp-10-10875-2010, 2010.

Müller, T., Henzing, J. S., de Leeuw, G., Wiedensohler, A., Alastuey, A., Angelov, H., Bizjak, M., Collaud Coen, M., Engström, J. E., Gruening, C., Hillamo, R., Hoffer, A., Imre, K.,Ivanow, P., Jennings, G., Sun, J. Y., Kalivitis, N., Karlsson, H.,Komppula, M., Laj, P., Li, S.-M., Lunder, C., Marinoni, A., Martins dos Santos, S., Moerman, M., Nowak, A., Ogren, J. A., Petzold,A., Pichon, J. M., Rodriquez, S., Sharma, S., Sheridan, P. J., Teinilä, K., Tuch, T., Viana, M., Virkkula, A., Weingartner, E., Wilhelm, R., and Wang, Y. Q.: Characterization and intercomparison of aerosol absorption photometers: result of two intercomparison workshops, Atmos. Meas. Tech., 4, 245–268, doi:10.5194/amt-4-245-2011, 2011.

Novakov, T.: The role of soot and primary oxidants in atmospheric chemistry, Science of the Total Environment, 36, 1–10, doi:10.1016/0048-9697(84)90241-9, 1984.

Nyeki, S., Baltensperger, U., Colbeck, I., Jost, D. T., Weingartner, E., and Gäggeler, H. W.: The Jungfraujoch high-alpine research station (3454 m) as a background clean continental site for the measurement of aerosol parameters, J. Geophys. Res., 103, 6097–6107, 1998.

Ohmura, A., Dutton, E. G., Forgan, B., Fröhlich, C., Gilgen, H., Hegner, H., Heimo, A., König-Langlo, G., McArthur, B., Müller, G., Philipona, R., Pinker, R., Whitlock, C. H., Dehne, K., and Wild, M.: Baseline Surface Radiation Network (BSRN/WCRP): New Precision Radiometry for Climate Research, B. Am. Meteor. Soc., 79, 2115–2136, 1998.

Pereira, E. B., Evangelista, H., Pereira, K. C. D., Cavalcanti, I. F. A., and Setzer, A.: Apportionment of black carbon in the South Shetland Islands, Antarctic Peninsula, J. Geophys. Res., 111, D03303, doi:10.1029/2005JD006086, 2006.

Petzold, A. and Schönlinner, M.: Multi-angle absorption photometry – a new method for the measurement of aerosol light absorption and atmospheric black carbon, J. Aerosol Sci., 35, 421–441, 2004.

Petzold, A., Kopp, C., and Niessner, R.: The dependence of the specific attenuation cross-section on black carbon mass fraction and particle size, Atmos. Environ., 31, 661–672, 1997.

Petzold, A., Schloesser, H., Sheridan, P. J., Arnott, W. P., Ogren, J. A., and Virkkula, A.: Evaluation of Multiangle Absorption Photometry for Measuring Aerosol Light Absorption, Aerosol Sci. Technol., 39, 40–51, doi:10.1080/027868290901945, 2005

Petzold, A., Rasp, K., Weinzierl, B., Esselborn, M., Hamburger, T., Dörnbrack, A., Kandler, K., Schütz, L., Knippertz, P., Fiebig, M., and Virkkula, A.: Saharan dust absorption and refractive index from aircraft-based observations during SAMUM 2006, Tellus, B61, 118–130, doi:10.1111/j.1600-0889.2008.00383.x, 2009.

Petzold, A., Veira, A., Mund, S., Esselborn, M., Kiemle, C., Weinzierl, B., Hamburger, T., Ehret, G., Lieke, K., and Kandler, K.: Mixing of mineral dust with urban pollution aerosol over Dakar (Senegal): Impact on dust physico-chemical and radiative properties, Tellus, B63, 619–634, doi:10.1111/j.1600-0889.2011.00547.x, 2011.

Pirazzini, R.: Surface albedo measurements over Antarctic sites in summer, J. Geophys. Res., 109, D20118, doi:10.1029/2004JD004617, 2004.

Ramanathan, V., Crutzen, P. J., Kiehl, J. T., and Rosenfeld, D.: Aerosols, Climate, and the Hydrological Cycle, Science, 294, 2119–2124, 2001.

Sanak, J., Gaudry, A., and Lambert, G.: Size distribution of $^{210}$Pb aerosols over oceans, Geophys. Res. Lett., 8, 1067–1069, 1981.

Schnaiter, M., Horvath, H., Möhler, O., Naumann, K.-H., Saathoff, H., Schöck, O. W.: UV-VIS-NIR spectral optical properties of soot and soot-containing aerosols, J. Aerosol Sci., 34, 1421–1444, 2003.

Seinfeld, J.: Black carbon and brown clouds, Nature Geosci., 1, 15–16, 2008.

Seinfeld, J. H. and Pandis, S. N.: Atmospheric Chemistry and Physics, From Air Pollution to Climate Change, 2nd ed., 628–635, John Wiley & Sons, Hoboken, NJ, USA, 2006a.

Seinfeld, J. H. and Pandis, S. N.: Atmospheric Chemistry and Physics, From Air Pollution to Climate Change, 2nd ed., 1060–1062, John Wiley, Hoboken, NJ, USA, 2006b.

Shirsat, S. V. and Graf, H. F.: An emission inventory of sulphur from anthropogenic sources in Antarctica, Atmos. Chem. Phys., 9, 3397–3408, doi:10.5194/acp-9-3397-2009, 2009.

Smith, J., Vance, D., Kemp, R. A, Archer, C., Toms, P., King, M., and Zárate, M.: Isotopic constraints on the source of Argentinean loess – with implications for atmospheric circula-tion and the provenance of Antarctic dust during recent glacial maxima, Earth Planet. Sci. Lett., 212, 181–196, 2003.

Stohl, A. and Sodeman, H.: Characteristics of atmospheric transport into the Antarctic troposphere, J. Geophys. Res., 115, D02305, doi:10.1029/2009JD012536, 2010.

Van de Berg, W. J., van den Broeke, M. R., and van Meijgaard, E.: Heat budget of the East Antarctic lower atmosphere derived from a regional atmospheric climate model, J. Geophys. Res., 112, D23101, doi:10.1029/2007JD008613, 2007.

Van der Werf, G. R., Randerson, J. T., Giglio, L., Collatz, G. J., Kasibhatla, P.S., and Arellano Jr., A. F.: Interannual variability in global biomass burning emissions from 1997 to 2004, Atmos. Chem. Phys., 6, 3423–3441, doi:10.5194/acp-6-3423-2006, 2006.

Van der Werf, G. R., Randerson, J. T., Giglio, L., Gobron, N., and Dolman, A. J.: Climate controls on the variability of fires in the tropics and subtropics, Global Biogeochem. Cy., 22, GB3028, doi:10.1029/2007GB003122, 2008.

Wagenbach, D., Görlach, U., Moser, K., and Münnich, K. O.: Coastal Antarctic aerosol: the seasonal pattern of its chemical composition and radionuclide content, Tellus, 40B, 423–436, 1988.

Warren, S. G. and Clarke, A. D.: Soot in the atmosphere and snow surface of Antarctica, J. Geophys. Res., 95, 1811–1816, 1990.

Weingartner, E., Saathoff, H., Schnaiter, M., Streit, N., Bitnar, B., and Baltensperger, U.: Absorption of light by soot particles: Determination of the absorption coefficient by means of Aethalometers, J. Aerosol Sci., 34, 1445–1465, 2003.

Weller, R. and Lampert, A.: Optical properties and sulfate scattering efficiency of boundary layer aerosol at coastal Neu-

mayer Station, Antarctica, J. Geophys. Res., 113, D16208, doi:10.1029/2008JD009962, 2008.

Weller, R., Wöltjen, J., Piel, C., Resenberg, R., Wagenbach, D., König-Langlo, G., and Kriews, M.: Seasonal variability of crustal and marine trace elements in the aerosol at Neumayer station, Antarctica, Tellus, 60B, 742–752, doi:10.1111/j.1600-0889.2008.00372.x, 2008.

Wolff, E. W. and Cachier, H.: Concentrations and seasonal cycle of black carbon in aerosol at a coastal Antarctic station, J. Geophys. Res., 103, 11033–11041, 1998.

Wuttke, S., Seckmeyer, G., and König-Langlo, G.: Measurements of spectral snow albedo at Neumayer, Antarctica, Ann. Geophys., 24, 7–21, doi:10.5194/angeo-24-7-2006, 2006.